

Lyman- α limit on axion-like cold dark matter

Zixuan Xu and Sibozheng

Department of Physics, Chongqing University, Chongqing 401331, China

Abstract

Using low redshift data on astrophysical reionization, we report new Lyman- α limit on axion-like particle (ALP) as cold dark matter in ALP mass range of $m_a \sim 30 - 1000$ eV. Compared to the Leo T and soft-X ray bound, this limit is so far the most stringent in the ALP mass range of $m_a \sim 375 - 425$ eV and complementary in the ALP mass range otherwise. Combining these limits, we show new exclusion limits on m_a for the ALP DM from either misalignment or freeze-in mechanism.

Contents

1	Introduction	1
2	Lyman-α limit	2
3	Implications to ALP dark matter	4
4	Conclusion	7

1 Introduction

Dark matter (DM) has shown its existence through gravitational interactions. To uncover the particle nature of DM, various experiments aiming to detect both weakly interacting massive particle (WIMP) and non-WIMP have been put in place. For the later there are several examples including millicharged particle [1–3], sterile neutrino [4–7], scalar [8], and QCD axion [9–12] to solve the strong CP problem. A common feature of these hypothetical particles is a feeble coupling to the Standard Model (SM), which allows them to hide in parameter regions beyond conventional experimental reaches.

Astrophysical and cosmic rays are few of tools being applicable to test non WIMP-like DM. For DM mass larger than \sim keV scale, X/γ -rays [13–16] due to DM decays inside specified galaxies cannot exceed the known backgrounds. For DM mass above \sim eV scale, observations of cosmic rays including Lyman- α forest and 21-cm signal provide data about temperature and reionization of the intergalactic medium (IGM), allowing us to place constraints on DM annihilation or decay into photons or electron-positron pair. So far, cosmic rays have been mainly used to constrain DM with mass above keV scale. Refs.[17–19] show that current Lyman- α data has already excluded DM lifetime (cross section of annihilation into electron-positron) smaller (larger) than $\sim 10^{25} - 10^{26}$ sec ($10^{-30} - 10^{-28}$ cm³s⁻¹). Refs.[19–22] show that future sensitivities of 21-cm signal can provide stronger constraints than the Lyman- α forest.

In practice, the cosmic rays are more useful to probe DM with mass below keV scale such as axion-like particle (ALP) - an extension of QCD axion. See e.g. [23, 24] for reviews. In this work, we report new Lyman- α limit on the ALP DM within ALP mass range of eV - keV. Starting with the ALP interactive Lagrangian

$$\mathcal{L}_{\text{eff}} = -\frac{g_{a\gamma\gamma}}{4} a F_{\mu\nu} \tilde{F}^{\mu\nu} + \dots, \quad (1)$$

where a is the ALP and F is the electromagnetic field strength respectively, one obtains the ALP lifetime

$$\tau_a \approx 8.5 \times 10^{35} \text{sec} \left(\frac{g_{a\gamma\gamma}}{10^{-10} \text{GeV}} \right)^{-2} \left(\frac{m_a}{250 \mu\text{eV}} \right)^{-3}, \quad (2)$$

where interactions neglected in eq.(1) do not affect the value of τ_a in the ALP mass range of $m_a < 2m_e$ considered here. Eq.(2) points to τ_a ranging from 10^{25} sec to 10^{30} sec in parameter regions with $g_{a\gamma\gamma} \sim 10^{-12} - 10^{-11}$ GeV⁻¹ and $m_a \sim 1 - 10^3$ eV, which are not yet excluded by

current experiments limits. We will show that these parameter regions are in the reach of current Lyman- α data, and uncover the physical implications to the ALP DM from either misalignment [25–28] or freeze-in mechanisms [29].

2 Lyman- α limit

Stimulation. In the late-time Universe the evolution of IGM ionization fraction and temperature is described by [30]

$$\frac{dx_{\text{HII}}}{dz} = \frac{dt}{dz} (\Lambda_{\text{ion}} - \Lambda_{\text{rec}} + \Lambda_{\text{ion}}^{\text{DM}}), \quad (3)$$

$$\frac{dT_k}{dz} = \frac{2 T_k}{3 n_b} \frac{dn_b}{dz} - \frac{T_k}{1 + x_e} \frac{dx_e}{dz} + \frac{2}{3 k_B (1 + x_e)} \frac{dt}{dz} \left(\sum_p \epsilon_{\text{heat}}^p + \epsilon_{\text{heat}}^{\text{DM}} \right), \quad (4)$$

respectively, where $x_{\text{HII}} = n_{H^+}/n_H$ is the ionization fraction with n_H (n_{H^+}) the number density of (ionized) hydrogen, T_k the matter (baryon) temperature, n_b the baryon number density, k_B the Boltzmann constant, z the redshift, Λ_{ion} the ionization rate, Λ_{rec} the recombination rate, ϵ_{heat}^p the Compton scattering and astrophysical source induced heating rate.

The ALP DM decay induced terms in eqs.(3) and (4) are given by [30]

$$\Lambda_{\text{ion}}^{\text{DM}} = \mathcal{F}_H \frac{\epsilon_{\text{HII}}^{\text{DM}}}{E_{\text{th}}^{\text{HI}}} + \mathcal{F}_{\text{He}} \frac{\epsilon_{\text{HeII}}^{\text{DM}}}{E_{\text{th}}^{\text{HeI}}}, \quad (5)$$

$$\epsilon_c^{\text{DM}} = f_c(x_e, z) \frac{1}{n_b} \left(\frac{dE(z)}{dt dV} \right)_{\text{inj}}, \quad (6)$$

where $f_c(x_e, z)$ are the deposition fractions, with deposition channels including IGM heating ($c=\text{heat}$), hydrogen ionization ($c = \text{HII}$), helium single or double ionization ($c = \text{HeII}$ or HeIII), and neutral atom excitation ($c = \text{exc}$), \mathcal{F}_j refers to the number fraction of each species j , E_{th}^j is the energy for ionization, and the DM induced energy injection rate is

$$\left(\frac{dE(z)}{dt dV} \right)_{\text{inj}} = \frac{\rho_{\text{DM},0} (1+z)^3}{\tau_a}, \quad (7)$$

with $\rho_{\text{DM},0}$ the observed DM relic density.

Using the publicly available package `DarkHistory` [30], we calculate the DM decay induced effects on the evolution of IGM parameters with m_a and τ_a as free input parameters.

Data. Reionization is believed to occur due to the astrophysical source. Therefore the data [31, 32] about T_k in the low redshift range of $z \sim 4 - 7$, together with the Planck data [33] about x_e , allows us to fix the astrophysical contribution in eqs.(3) and (4). To do so, we follow [18] to adopt the FlexKnot model to parametrize the astrophysical source contribution to Λ_{ion} in eq.(3) and photoheated prescription to parametrize the astrophysical source contribution to ϵ_{heat}^p in eq.(4), respectively. Given the astrophysical reionization established, it is straightforward to carry out the Lyman- α limit on the DM induced effects on the IGM parameters.

Comparison with existing bounds. Fig.1 shows the new Lyman- α limit on the plane of (m_a, τ_a) , compared to the other existing bounds in the literature. Three comments are in order:

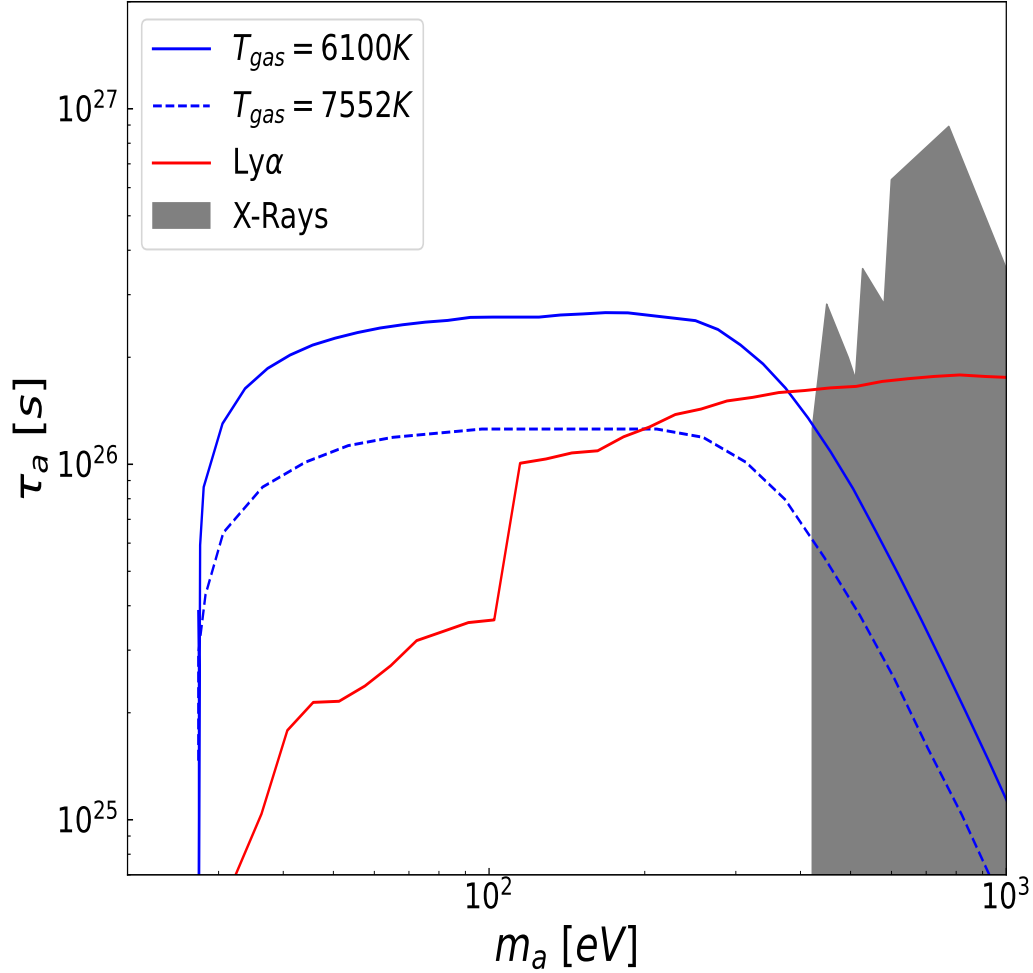


Figure 1: Lyman- α limit on the plane of (m_a, τ_a) at 95% CL, where regions below the red curve are excluded. For a comparison we have shown the other existing bounds including soft X-ray [13] recasted from [34, 35] in shaded region, and Leo T [36] with two reference values of T_{gas} in blue. See text for details.

- Compared to reported Lyman- α limits [18, 19] across the mass range of $m_a \geq \text{keV}$, we have extended it (in red) down to the mass range of $m_a \sim 30 \text{ eV}$ in fig.1. Note, this limit is absent in smaller m_a region, as the DM decay induced photon energy E_γ has to exceed the threshold value of $\sim 10.2 \text{ eV}$ to heat the IGM.
- For $m_a \sim 30 - 375 \text{ eV}$, the Lyman- α limit is comparable with the Leo T bound [36] (in green) depending on the temperature of gas in Leo T, where we have used two reference values of $T_{\text{gas}} = \{6100, 7552\} \text{ K}$ for illustration.

- For $m_a \sim 375 - 425$ eV, our result is the most stringent.
- For $m_a \sim 425 - 1000$ eV, this limit is complementary to soft X-ray bound [13] (in shaded region) derived from [34, 35].

To summarize, the Lyman- α limit is the most stringent in the ALP mass range of $m_a \sim 375 - 425$ eV and complementary to the Leo T and soft X-ray bound in the ALP mass range otherwise.

3 Implications to ALP dark matter

Despite being insensitive to QCD axion DM whose surviving parameter region lies around $m_a \ll 1$ eV, the Leo T, soft-X ray and Lyman- α limit in fig.1 have important physical implications to the ALP DM with mass $m_a \sim 30 - 1000$ eV under consideration.

Misalignment mechanism. Under the context of misalignment mechanism [25–28], the ALP relic abundance is given by [38]

$$\Omega_a h^2 \sim 0.1 \left(\frac{m_a}{\text{eV}} \right)^{1/2} \left(\frac{f_a}{10^{11} \text{GeV}} \right)^2 \left(\frac{m_a}{m_a(t_*)} \right)^{1/2}, \quad (8)$$

where $g_{a\gamma\gamma} = (\alpha/2\pi)f_a^{-1}$ with f_a the broken scale of global $U(1)$ symmetry,

$$\frac{m_a}{m_a(t_*)} = \left(\frac{\Lambda}{T(t_*)} \right)^\beta, \quad (9)$$

with $m_a(t)$ the effective ALP mass depending on time t , t_* refers to the moment when $m_a(t_*) = 3H$ with H the Hubble rate, $\Lambda \approx m_a f_a$ is the characteristic mass scale of unbroken $SU(N)$ gauge group, T is the temperature of this new sector, and β is a dimensionless parameter. Eq.(8) suggests that the observed DM relic density can be addressed in the parameter regions with $m_a \sim 1 - 10^3$ eV and $g_{a\gamma\gamma} \sim 10^{-15} - 10^{-11} \text{ GeV}^{-1}$ depending on the value of β .

Fig.2 presents the constraints on the ALP DM from the misalignment mechanism, where the new Lyman- α limit in fig.1 is converted to the plane of $(m_a, g_{a\gamma\gamma})$ using eq.(2), and the black lines refer to the values of $\beta = \{0, 1, 3, 5, 7, 9\}$ from bottom to top. Compared to the earlier exclusion results $m_a \leq \{400, 380, 90\}$ eV [38] with respect to $\beta = \{0, 1, 3\}$ respectively made by ionization of primordial hydrogen (x_{ion} in green) and soft X-ray [13] (in gray) bound, they are updated to $m_a \leq \{110 - 140, 50 - 80, 30 - 45\}$ eV with respect to $\beta = \{0, 1, 3\}$ respectively in light of Leo T (in blue) and Lyman- α (in red) limit. These values can be further improved by near future data of Lyman- α forest and 21-cm signal.

Freeze – in mechanism. Apart from the misalignment mechanism, the ALP DM can be also produced via the freeze-in mechanism [29]. Given $g_{a\gamma\gamma}$ coupling, the ALP relic abundance arises from Primakoff process $q\gamma \rightarrow qa$ where q the SM charged fermions and inverse decay of $a \rightarrow \gamma\gamma$. The former is ultraviolet dominated being sensitive to reheating temperature T_{reh} , whereas the later is infrared dominated being independent on T_{reh} . For $m_a \ll \text{MeV}$ and $T_{\text{reh}} \gg 10 \text{ MeV}$ considered here, the former dominates over the later [39, 40].

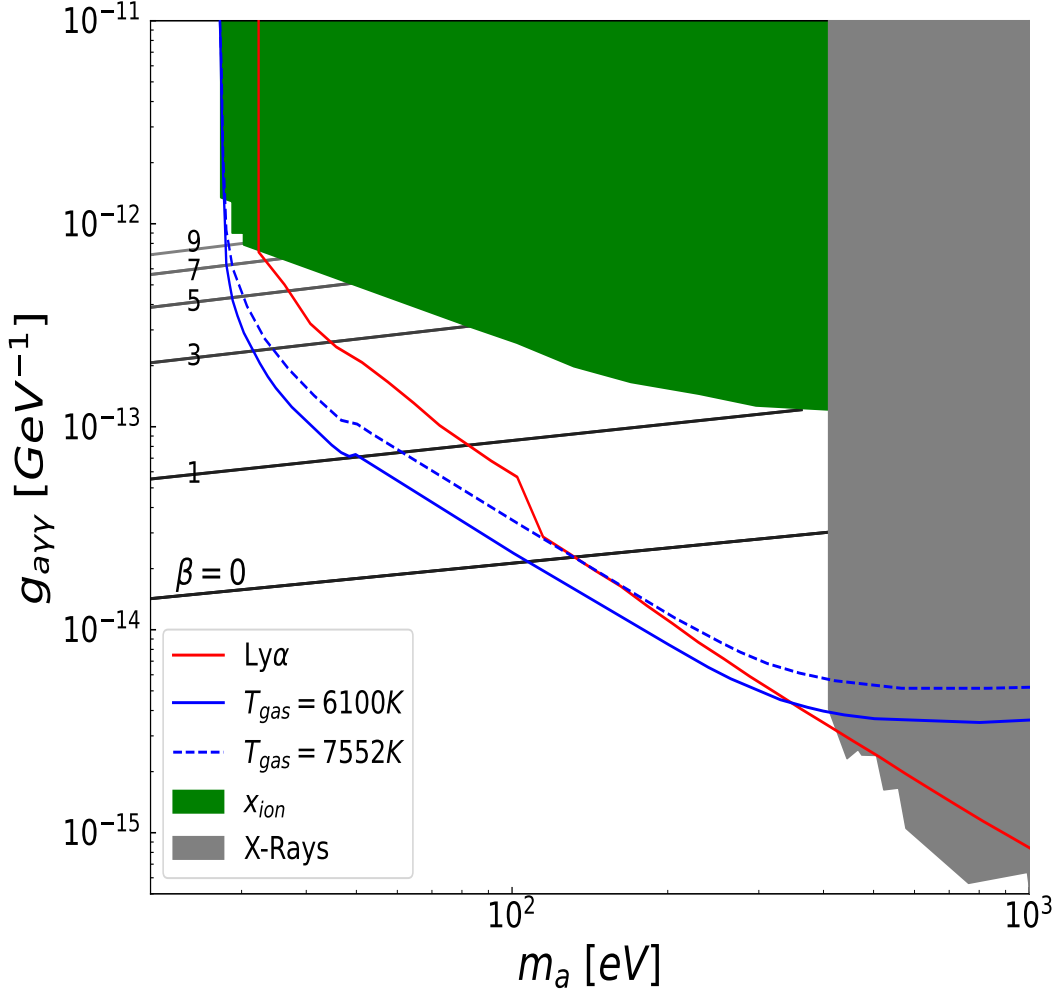


Figure 2: Constraint on the ALP DM through the misalignment mechanism, compared to current experimental bounds from x_{ion} [13] (in green), soft X-ray [13] (in gray), Leo T [36] (in blue), and Lyman- α forest (in red). The black lines correspond to the values of $\beta = \{0, 1, 3, 5, 7, 9\}$ from bottom to top. For a complete list of limits, see [37].

Neglecting the inverse decay contribution, the ALP relic abundance due to the Primakoff process is given by

$$\Omega_a h^2 \approx 4.5 \times 10^{-5} \left(\frac{g_{a\gamma\gamma}}{10^{-11} \text{ GeV}^{-1}} \right)^2 \left(\frac{m_a}{0.1 \text{ MeV}} \right) \left(\frac{T_{\text{reh}}}{10 \text{ MeV}} \right) \quad (10)$$

by scaling the result of [39]. The reheating temperature in eq.(10) is upper bounded as [13]

$$T_{\text{reh}} < T_{\text{fo}} \approx 10^5 \left(\frac{g_{a\gamma\gamma}}{10^{-11} \text{ GeV}^{-1}} \right)^{-2} \text{ GeV}, \quad (11)$$

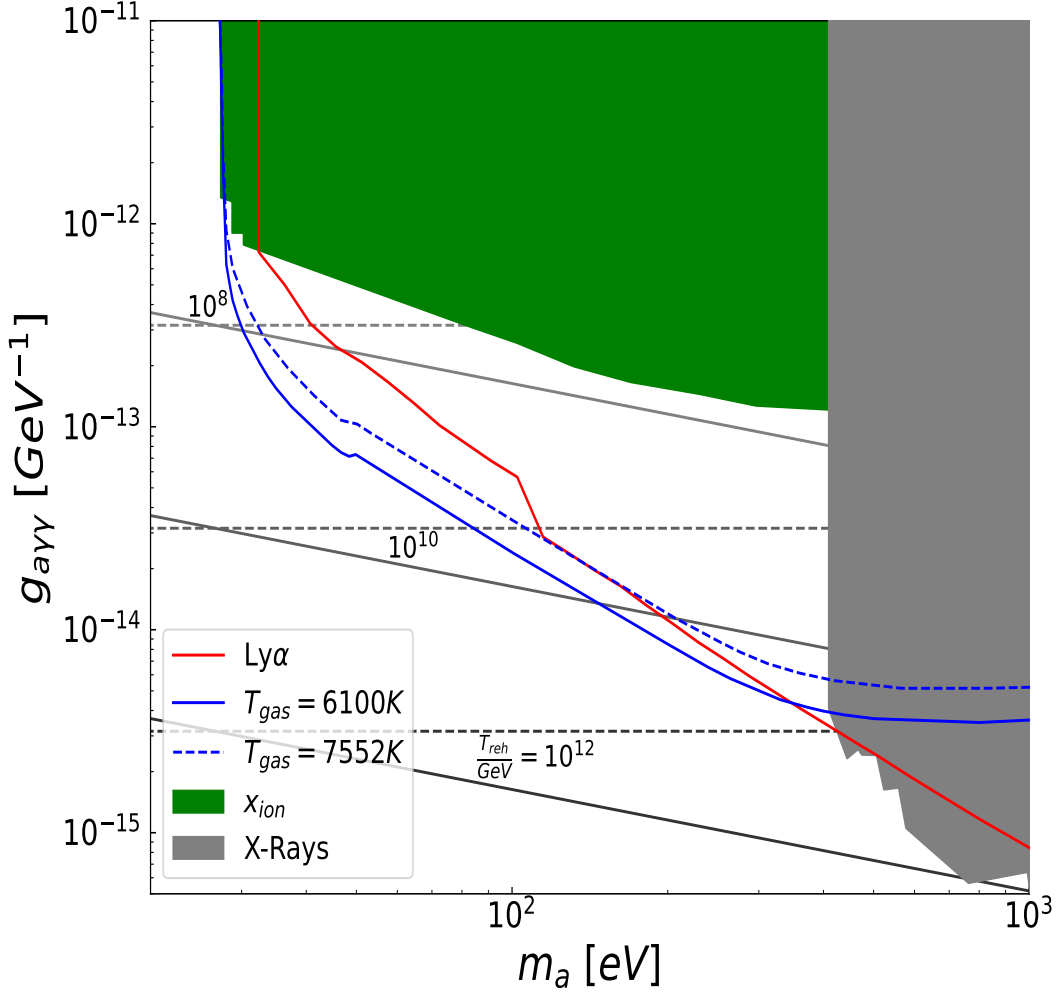


Figure 3: Same as in fig.2 but for the freeze-in mechanism. The solid gray lines refer to the observed DM relic abundance for various values of $T_{\text{reh}} = \{10^8, 10^{10}, 10^{12}\}$ GeV from top to bottom. The dotted gray lines refer to the freeze-in condition in eq.(11) with different values of T_{reh} , above which the solid lines are excluded.

where T_{fo} is the freeze-out temperature. Eq.(10) shows that the observed value of DM relic density can be addressed by $g_{a\gamma\gamma} \sim 10^{-15} - 10^{-11}$ GeV^{-1} and $m_a \sim 1 - 1000$ eV depending on the value of T_{reh} .

Fig.3 shows the observed DM relic abundance (in solid gray) projected to the plane of $m_a - g_{a\gamma\gamma}$ for various values of $T_{\text{reh}} = \{10^8, 10^{10}, 10^{12}\}$ GeV, which are compared to current experimental bounds and the freeze-in condition in eq.(11) (in dotted gray). With respect to each T_{reh} , the solid gray line above the dotted gray line is excluded. For T_{reh} lower than 10^{12} GeV, the combination of Leo T and Lyman- α limit implies $m_a \leq \{30 - 35, 155 - 205\}$ eV for $T_{\text{reh}} = \{10^8, 10^{10}\}$ GeV,

respectively. For T_{reh} higher than $\sim 10^{12}$ GeV, the entire mass range considered is beyond the reaches of all current limits. To be clarify, we remind the reader that ALP DM mass regions with $m_a < 1$ eV can be additionally excluded by limits not displayed in fig.3, a complete list of which can be found in ref.[37].

4 Conclusion

In this work we have presented the new Lyman- α limit within the DM mass range of $m_a \sim 30 - 1000$ eV. It has been shown to be the most stringent in the ALP DM mass range of $m_a \sim 375 - 425$ eV and complementary in the otherwise ALP DM mass range, compared to the Leo T and soft-X ray limit. Using these limits, we have excluded (i) the ALP DM mass down to $m_a/\text{eV} \sim 110 - 140, 50 - 80, 30 - 45$ eV for the parameter $\beta = 0, 1, 3$ respectively in the context of misalignment mechanism, and (ii) the ALP DM mass down to $m_a/\text{eV} \sim 30 - 35, 155 - 205$ for the reheating temperature $T_{\text{reh}}/\text{GeV} = 10^8, 10^{10}$ respectively in the context of freeze-in mechanism.

References

- [1] B. Holdom, Phys. Lett. B **166**, 196-198 (1986).
- [2] D. Feldman, Z. Liu and P. Nath, Phys. Rev. D **75**, 115001 (2007), [arXiv:hep-ph/0702123 [hep-ph]].
- [3] X. Yin, S. Xu and S. Zheng, [arXiv:2311.10360 [hep-ph]].
- [4] T. Asaka, K. Ishiwata and T. Moroi, Phys. Rev. D **73**, 051301 (2006), [arXiv:hep-ph/0512118 [hep-ph]].
- [5] M. Becker, Eur. Phys. J. C **79**, no.7, 611 (2019), [arXiv:1806.08579 [hep-ph]].
- [6] M. Chianese and S. F. King, JCAP **09**, 027 (2018), [arXiv:1806.10606 [hep-ph]].
- [7] A. Datta, R. Roshan and A. Sil, Phys. Rev. Lett. **127**, no.23, 231801 (2021), [arXiv:2104.02030 [hep-ph]].
- [8] J. McDonald, Phys. Rev. Lett. **88**, 091304 (2002), [arXiv:hep-ph/0106249 [hep-ph]].
- [9] R. D. Peccei and H. R. Quinn, Phys. Rev. Lett. **38**, 1440-1443 (1977).
- [10] R. D. Peccei and H. R. Quinn, Phys. Rev. D **16**, 1791-1797 (1977).
- [11] S. Weinberg, Phys. Rev. Lett. **40**, 223-226 (1978).
- [12] F. Wilczek, Phys. Rev. Lett. **40**, 279-282 (1978).
- [13] D. Cadamuro and J. Redondo, JCAP **02**, 032 (2012), [arXiv:1110.2895 [hep-ph]].
- [14] G. Vertongen and C. Weniger, JCAP **05**, 027 (2011), [arXiv:1101.2610 [hep-ph]].
- [15] R. Essig, E. Kuflik, S. D. McDermott, T. Volansky and K. M. Zurek, JHEP **11**, 193 (2013), [arXiv:1309.4091 [hep-ph]].

- [16] T. Cohen, K. Murase, N. L. Rodd, B. R. Safdi and Y. Soreq, Phys. Rev. Lett. **119**, no.2, 021102 (2017), [arXiv:1612.05638 [hep-ph]].
- [17] H. Liu, T. R. Slatyer and J. Zavala, Phys. Rev. D **94** (2016) no.6, 063507, [arXiv:1604.02457 [astro-ph.CO]].
- [18] H. Liu, W. Qin, G. W. Ridgway and T. R. Slatyer, Phys. Rev. D **104**, no.4, 043514 (2021), [arXiv:2008.01084 [astro-ph.CO]].
- [19] Z. Xu, Q. Zhou and S. Zheng, [arXiv:2407.08225 [hep-ph]].
- [20] Y. Sun, J. W. Foster, H. Liu, J. B. Muñoz and T. R. Slatyer, [arXiv:2312.11608 [hep-ph]].
- [21] G. Facchinetti, L. Lopez-Honorez, Y. Qin and A. Mesinger, [arXiv:2308.16656 [astro-ph.CO]].
- [22] A. Mitridate and A. Podo, JCAP **05** (2018), 069, [arXiv:1803.11169 [hep-ph]].
- [23] D. J. E. Marsh, Phys. Rept. **643**, 1-79 (2016), [arXiv:1510.07633 [astro-ph.CO]].
- [24] C. B. Adams, N. Aggarwal, A. Agrawal, R. Balafendiev, C. Bartram, M. Baryakhtar, H. Bekker, P. Belov, K. K. Berggren and A. Berlin, *et al.* [arXiv:2203.14923 [hep-ex]].
- [25] L. F. Abbott and P. Sikivie, Phys. Lett. B **120**, 133-136 (1983).
- [26] J. Preskill, M. B. Wise and F. Wilczek, Phys. Lett. B **120**, 127-132 (1983).
- [27] M. Dine and W. Fischler, Phys. Lett. B **120**, 137-141 (1983).
- [28] M. S. Turner, Phys. Rev. D **28**, 1243 (1983).
- [29] L. J. Hall, K. Jedamzik, J. March-Russell and S. M. West, JHEP **03**, 080 (2010), [arXiv:0911.1120 [hep-ph]].
- [30] H. Liu, G. W. Ridgway and T. R. Slatyer, Phys. Rev. D **101**, no.2, 023530 (2020), [arXiv:1904.09296 [astro-ph.CO]].
- [31] M. Walther, J. Oñorbe, J. F. Hennawi and Z. Lukić, Astrophys. J. **872** (2019) no.1, 13, [arXiv:1808.04367 [astro-ph.CO]].
- [32] P. Gaikwad, M. Rauch, M. G. Haehnelt, E. Puchwein, J. S. Bolton, L. C. Keating, G. Kulkarni, V. Iršič, E. Bañados and G. D. Becker, *et al.* Mon. Not. Roy. Astron. Soc. **494** (2020) no.4, 5091-5109, [arXiv:2001.10018 [astro-ph.CO]].
- [33] N. Aghanim *et al.* [Planck], Astron. Astrophys. **641**, A6 (2020) [erratum: Astron. Astrophys. **652**, C4 (2021)], [arXiv:1807.06209 [astro-ph.CO]].
- [34] A. Boyarsky, A. Neronov, O. Ruchayskiy, M. Shaposhnikov and I. Tkachev, Phys. Rev. Lett. **97**, 261302 (2006), [arXiv:astro-ph/0603660 [astro-ph]].
- [35] A. Boyarsky, O. Ruchayskiy and M. Shaposhnikov, Ann. Rev. Nucl. Part. Sci. **59**, 191-214 (2009), [arXiv:0901.0011 [hep-ph]].
- [36] D. Wadekar and Z. Wang, Phys. Rev. D **106**, no.7, 075007 (2022), [arXiv:2111.08025 [hep-ph]].

- [37] C. O'Hare, cajohare/axionlimits: Axionlimits, <https://cajohare.github.io/AxionLimits/>, July, 2020.
- [38] P. Arias, D. Cadamuro, M. Goodsell, J. Jaeckel, J. Redondo and A. Ringwald, JCAP **06**, 013 (2012), [arXiv:1201.5902 [hep-ph]].
- [39] M. Jain, A. Maggi, W. Y. Ai and D. J. E. Marsh, [arXiv:2406.01678 [hep-ph]].
- [40] K. Langhoff, N. J. Outmezguine and N. L. Rodd, Phys. Rev. Lett. **129**, no.24, 241101 (2022), [arXiv:2209.06216 [hep-ph]].